

Fractional Cable Models for Spiny Neuronal Dendrites

B. I. Henry* and T. A. M. Langlands†

Department of Applied Mathematics, School of Mathematics, University of New South Wales, Sydney NSW 2052, Australia

S. L. Wearne‡

Laboratory of Biomathematics, Department of Neuroscience, Mount Sinai School of Medicine, New York, New York 10029-6574, USA

(Received 9 September 2007; published 28 March 2008)

Cable equations with fractional order temporal operators are introduced to model electrotonic properties of spiny neuronal dendrites. These equations are derived from Nernst-Planck equations with fractional order operators to model the anomalous subdiffusion that arises from trapping properties of dendritic spines. The fractional cable models predict that postsynaptic potentials propagating along dendrites with larger spine densities can arrive at the soma faster and be sustained at higher levels over longer times. Calibration and validation of the models should provide new insight into the functional implications of altered neuronal spine densities, a hallmark of normal aging and many neurodegenerative disorders.

DOI: [10.1103/PhysRevLett.100.128103](https://doi.org/10.1103/PhysRevLett.100.128103)

PACS numbers: 87.19.L-, 05.40.-a, 87.16.A-

Most of the brain's gray matter is composed of spiny dendrites. Dendritic processes respond to synaptic inputs by relaying postsynaptic potentials to the cell body or soma. The potentials are summed at the soma and the cell fires an action potential or spike if a threshold potential is exceeded. The interspike interval determines the firing rate of nerve cells which is critical for normal cognitive functioning. An ongoing dialogue between theory and experiments over many decades has revealed the detailed electrotonic properties of neuronal dendrites and dendritic trees [1]. The centerpiece of this is the cable equation [2,3]

$$r_m c_m \frac{\partial V}{\partial t} = \frac{dr_m}{4r_L} \frac{\partial^2 V}{\partial x^2} - V + r_m i_e, \quad (1)$$

which models the spatiotemporal evolution of the membrane potential V_m , relative to the resting membrane potential V_{rest} , along the axial x direction of a cylindrical nerve cell segment. The other parameters in the model represent the specific membrane resistance r_m , longitudinal resistivity r_L , membrane capacitance per unit area c_m , diameter d , and an external injected current per unit area i_e . In an infinite length cable described by Eq. (1) the steady state voltage attenuates in space by a factor $1/e$ over a distance of $\lambda = \sqrt{\frac{dr_m}{4r_L}}$ and the spatially homogeneous voltage for a membrane patch attenuates in time by a factor $1/e$ over a time $\tau = r_m c_m$, so that λ and τ are referred to as the space constant and the time constant for the dendrite. The cable equation can be obtained phenomenologically by associating electrical properties with the cell membrane [3] or derived physically from the Nernst-Planck equation for electrodiffusive motion of ions [4].

Over the past few decades research on neuronal dendrites has intensified [5] due to the discovery that dendrites are highly active, with complex electrical and biochemical signaling depending on both local spine structure and density [6,7], and on voltage-gated ion channels [8]. These processes present challenges to the cable model

[9]. In this Letter we consider refinements of the passive cable model (voltage-gated ion channels are ignored) to incorporate dendritic spines (small protrusions extending out from dendritic branches) [7,9]. The standard way to model the effects of spines in the passive cable model is to reduce the membrane resistance and to increase the membrane capacitance, for an equivalent but smooth dendrite, by a factor proportional to the increased membrane surface area due to spines [9]. In this modification the time constant is unaffected by spines but the space constant is reduced; thus, the steady state voltage should attenuate more strongly in space along spiniar dendrites [9,10].

A recent study [11] on spiny Purkinje cell dendrites showed that spines trap and release diffusing molecules resulting in anomalously slow molecular diffusion, along the dendrite. The diffusive spatial variance $\langle r^2(t) \rangle$ of an inert tracer was found to evolve as a sublinear power law in time, i.e., $\langle r^2(t) \rangle \sim t^\alpha$ with $0 < \alpha < 1$. The diffusion became more anomalous (smaller α) with increasing spine density [11]. In this Letter we derive fractional cable equations from fractional Nernst-Planck equations, introduced to model anomalous electrodiffusion of ions in spiny dendrites, and we investigate the solutions of the fractional cable equations to provide new insights into the electrotonic effects of the trapping properties of spines.

The simplest model for anomalous diffusion replaces the diffusion constant D with a time-dependent diffusion coefficient $D\alpha t^{\alpha-1}$ in the standard diffusion equation. This models fractional Brownian motion (FBM) that can be derived from a Langevin equation with a friction memory kernel and power law correlated noise [12]. A different model for anomalous diffusion includes a temporal derivative with fractional order $1 - \alpha$ operating on the spatial Laplacian in the diffusion equation [13]. This fractional equation has been derived from mesoscopic continuous time random walks (CTRWs) with a power law waiting-time distribution $\psi(t) \sim t^{-(1+\alpha)}$ [13], characteristic of traps [14]. In the absence of experimental evidence to the con-

trary, it is prudent to consider both FBM and CTRW based anomalous diffusion models in fitting experiments [15,16].

The Nernst-Planck equation is the fundamental macroscopic model for the microscopic motions of ions in nerve cells. This model takes into account random motions of the ions as well as the drift of ions due to the electric field of the membrane potential (due to different ionic concentrations inside and outside the cell membrane). As a starting point, to model anomalous electrodiffusion, we consider the following variant of the Nernst-Planck equation:

$$\frac{\partial C_k}{\partial t} = \mathcal{D}_k(\gamma_k, t) \nabla^2 C_k + \nabla \cdot \left(\frac{z_k F}{RT} \mathcal{D}_k(\gamma_k, t) C_k \nabla V_m \right). \quad (2)$$

In this equation, C_k is the concentration of the k th ionic species, F is the Faraday constant, R is the universal gas constant, and T is the temperature. The difference between this model and the standard Nernst-Planck equation is that $\mathcal{D}_k(\gamma_k, t)$ is not a constant for a given species k but is a parametrized time-dependent operator with scaling parameter $0 < \gamma_k \leq 1$. As discussed above we consider the two possibilities related to FBM and CTRWs, respectively:

(i)

$$\mathcal{D}_k(\gamma_k, t) = D_k(\gamma_k) \gamma_k t^{\gamma_k - 1} \quad (3)$$

where $D_k(\gamma_k)$ has units of $m^2 s^{-\gamma_k}$, and (ii)

$$\mathcal{D}_k(\gamma_k, t) = D_k(\gamma_k) \frac{\partial^{1-\gamma_k}}{\partial t^{1-\gamma_k}}, \quad (4)$$

where $\frac{\partial^{1-\gamma}}{\partial t^{1-\gamma}}$ is the Riemann-Liouville fractional derivative operator defined by

$$\frac{\partial^{1-\gamma}}{\partial t^{1-\gamma}} Y(t) = \frac{1}{\Gamma(\gamma)} \frac{\partial}{\partial t} \int_0^t \frac{Y(t')}{(t-t')^{1-\gamma}} dt'. \quad (5)$$

In the following it is also useful to define the ‘‘normalized’’ operators $\mathcal{D}^*(\gamma_k, t) = \mathcal{D}_k(\gamma_k, t)/D_k(\gamma_k)$. Importantly, in both the standard Nernst-Planck equation ($\gamma = 1$) and the fractional Nernst-Planck equations ($0 < \gamma < 1$) the effects of ionic diffusion are not isolated to the Laplacian term, but they are also manifest in the drift term, through the dependence on the diffusion ‘‘constant.’’ It follows that even if concentration gradients are sufficiently small for the Laplacian term to be neglected, alterations in the environment that affect ionic diffusion would also affect the drift term. A second point to note is that in the fractional Nernst-Planck models the electric field force is a function of the ionic concentrations. As a result these models cannot be derived from CTRWs via fractional Fokker-Planck equations with external time independent forces [17,18]. The fractional Nernst-Planck models do, however, capture this effect; variations in the time-dependent force field are driven by the same temporal operator that affects variations in the time-dependent ionic concentrations. This contrasts with the fractional Fokker-Planck equations with external time-dependent force fields where an effective temporal subordination of the external force to the random walks is not appropriate [19].

The standard passive cable equation for a cylindrical nerve cell segment, with diameter d much smaller than the length ℓ , has been derived by Qian and Sejnowski [4] from the standard Nernst-Planck equation. We follow this approach in deriving the fractional cable models for spiny dendrites. First we integrate Eq. (2) in axially symmetric cylindrical coordinates over the circular cross section of the neuron, with zero flux of ions at the center. This results in

$$\frac{\partial C_k}{\partial t} = \mathcal{D}^*(\gamma_k, t) \left\{ D_k(\gamma_k) \frac{\partial^2 C_k}{\partial x^2} + \frac{z_k F}{RT} \frac{\partial}{\partial x} \left(D_k(\gamma_k) C_k \frac{\partial V_m}{\partial x} \right) \right\} - \frac{4}{d} J_k \Big|_{r=d/2}, \quad (6)$$

where x is the longitudinal coordinate, r is the radial coordinate, and J_k denotes the radial flux of ionic species k across the membrane. As in the standard cable theory we model the membrane potential as [20]

$$V_m(x, t) = V_{\text{rest}} + \frac{Fd}{4c_m} \sum_k z_k [C_k(x, t) - C_{k,\text{rest}}], \quad (7)$$

where $C_{k,\text{rest}}$ is the resting concentration of the k th ionic species. We also follow the standard assumption that the axial ionic concentration gradients are small ($\partial C_k / \partial x \approx 0$), but the prefactor $\frac{Fd}{4c_m}$ is large ($\partial V_m / \partial x \neq 0$) [4]. In addition we assume that the trapping effects due to the geometry of spines are similar for different species of mobile ions ($\gamma_k \approx \gamma$). Using these results in Eq. (6) we obtain

$$c_m \frac{\partial V_m}{\partial t} = \mathcal{D}^*(\gamma, t) \left(\frac{d}{4r_L} \frac{\partial^2 V_m}{\partial x^2} \right) - i_m + i_e, \quad (8)$$

where

$$\frac{1}{r_L(\gamma)} = \frac{F^2}{RT} \sum_k z_k^2 D_k(\gamma) C_k \quad (9)$$

defines a modified longitudinal resistivity $r_L(\gamma)$ with units of $\Omega m s^{\gamma-1}$, $i_m = \sum_k z_k F J_k$ is the total ionic transmembrane current per unit area, and i_e has been included as an injected current per unit area.

As an alternative to the physical derivation above, the fractional cable equation, Eq. (8), can be obtained phenomenologically by combining the standard current continuity equation

$$c_m \frac{\partial V_m}{\partial t} = \frac{d}{4} \frac{\partial I_L}{\partial x} - i_m + i_e \quad (10)$$

with the longitudinal current I_L described by a fractional variant of Ohm’s law,

$$I_L = -\mathcal{D}^*(\gamma, t) \frac{1}{r_L(\gamma)} \frac{\partial V_m}{\partial x}. \quad (11)$$

Allowing for a similar fractional flux for the ionic transmembrane current, we write

$$i_m = \alpha(\kappa) \mathcal{D}^*(\kappa, t) \frac{V_m - V_{\text{rest}}}{r_m}, \quad (12)$$

where κ is the exponent characterizing the anomalous flux across the membrane and $\alpha(\kappa)$ is an additional parameter with units of $s^{1-\kappa}$. It is possible to absorb $\alpha(\kappa)$ into a modified specific membrane resistance $r_m(\kappa) = r_m/\alpha(\kappa)$, identifying $\alpha(\kappa)$ as the effect of anomalous flux across the channels on the specific membrane resistance, and $\alpha(1) = 1$. The fractional order operator $\mathcal{D}^*(\kappa, t)$ would also apply to any external current i_e carried by ions traversing the membrane. Equations (11) and (12) can be interpreted as either an aged linear response [21] or a retarded linear response [22], if $\mathcal{D}^*(\kappa, t)$ has the form of Eq. (3) or Eq. (4), respectively.

Equations (8) and (12) can be combined to arrive at the linear fractional cable equation

$$r_m c_m \frac{\partial V}{\partial t} = \frac{dr_m}{4r_L(\gamma)} \mathcal{D}^*(\gamma, t) \left(\frac{\partial^2 V}{\partial x^2} \right) - \alpha(\kappa) \mathcal{D}^*(\kappa, t) (V - r_m i_e), \quad (13)$$

where $V = V_m - V_{\text{rest}}$. The above model yields a nontrivial steady state solution if the exponents γ and κ are equal. To investigate further solutions of Eq. (13) it is useful to consider the explicit dimensionless forms, related to Eqs. (3) and (4), respectively:

$$\frac{\partial V_I}{\partial T} = \gamma T^{\gamma-1} \frac{\partial^2 V_I}{\partial X^2} - \mu^2 \kappa T^{\kappa-1} (V_I - i_e r_m) \quad (14)$$

and

$$\frac{\partial V_{II}}{\partial T} = \frac{\partial^{1-\gamma}}{\partial T^{1-\gamma}} \frac{\partial^2 V_{II}}{\partial X^2} - \mu^2 \frac{\partial^{1-\kappa}}{\partial T^{1-\kappa}} (V_{II} - i_e r_m), \quad (15)$$

where $T = \frac{t}{\tau_m}$ is the dimensionless time variable, $X = x \tau_m^{(1-\gamma)/2} / \sqrt{dr_m/4r_L}$ is the dimensionless space variable, $\mu^2 = \alpha(\kappa) \tau_m^{\kappa-1}$ is a dimensionless function of κ , and the subscripts I and II are used to differentiate the two anomalous diffusion models.

The fundamental solutions of Eqs. (14) and (15) in the case of infinite cables with no external current are as follows:

$$G_I(X, T) = \frac{1}{\sqrt{4\pi T^\gamma}} \exp\left(-\frac{X^2}{4T^\gamma} - \mu^2 T^\kappa\right) \quad (16)$$

and [24]

$$G_{II}(X, T) = \frac{1}{\sqrt{4\pi T^\gamma}} \times \sum_{j=0}^{\infty} \frac{(-\mu^2 T^\kappa)^j}{j!} H_{1,2}^{2,0} \left[\frac{X^2}{4T^\gamma} \left| \begin{matrix} (1 - \frac{\gamma}{2} + \kappa j, \gamma) \\ (0, 1), (\frac{1}{2} + j, 1) \end{matrix} \right. \right], \quad (17)$$

where H is a Fox function [13]. Both of these solutions reduce to the standard fundamental solution for an infinite cable in the case $\gamma = \kappa = 1$. In the remainder of this Letter we consider solutions for $\gamma = \kappa \neq 1$. Solutions with $\gamma \neq \kappa$ are described elsewhere [23]. $G_I(X, T)$ with $\gamma = \kappa$ is identical to the fundamental solution of the standard cable equation, but at a later time. By contrast $G_{II}(X, T)$ with

$\gamma = \kappa$ (see Fig. 1, left) is characterized by a sharp peak and a heavy tail and is subordinated to the fundamental solution of the standard cable equation [23]. In both fractional models the peak height $G(0, T)$ decreases more rapidly with decreasing γ at early times but this trend reverses at longer times. The crossover time occurs at $T = 1.0$ independent of γ for G_I but the crossover time increases with decreasing γ for G_{II} (see Fig. 1, right). The major long time effect of the anomalous electrodiffusion through the cytoplasm is to slow down the spreading of the membrane potential along the membrane.

The fundamental solutions in Eqs. (16) and (17) can be used to approximate the passive propagation of a potential $V(X, T) = G(X - X', T)$ at position X and time T along a spiny dendrite corresponding to an instantaneous injection of unit current at position $X = X'$ with initially $V(X, 0) = 0$. Other current injections are described in [23]. Considering $X = 0$ as the position at the soma, we have plotted $V(0, T)$ versus T in Fig. 2 for impulsive current injections at $X' = 1$ for a range of $\gamma = \kappa = 0.1, 0.2, \dots, 0.9, 1.0$. Common features in both fractional cable models are (i) the peak potential at the soma arrives earlier with decreasing γ and (ii) after the arrival of the peak, the potential initially attenuates more rapidly with decreasing γ but on longer time scales the potential is higher for decreasing γ . These features are consistent with the faster early time but slower long time spreading of the fundamental solution (cf. Fig. 1). Given that the anomalous diffusion exponent γ decreases monotonically with spine density [see Fig. 3(B) of [11]] these results are important for addressing the electrotonic significance of decreasing spine densities that are characteristics of aging [25,26], Down's syndrome [27], and other neurological disorders [6]. One interpretation of the results in Fig. 2, which are dependent on calibration and validation of the models (see below), is that an increased density of dendritic spines can serve to (i) compensate the time delay of postsynaptic potentials along dendrites and (ii) reduce the long time temporal attenuation of postsynaptic potentials.

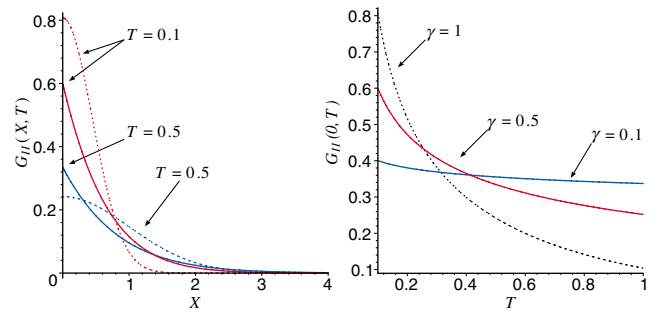


FIG. 1 (color online). Plots of $G_{II}(X, T)$ versus X (left) for $\gamma = \kappa = 0.5$ at the two times $T = 0.1$ and $T = 0.5$ and plots of $G_{II}(0, T)$ versus T (right) for $\gamma = \kappa = 0.5$, and $\gamma = \kappa = 0.1$. In both plots, the dashed lines show corresponding solutions of the standard cable equation $\gamma = \kappa = 1$.

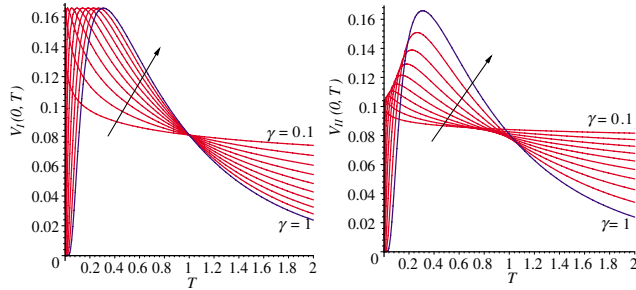


FIG. 2 (color online). Plots of $V_I(0, T)$ versus T (left) and $V_{II}(0, T)$ versus T (right) for $\gamma = \kappa = 0.1, 0.2, 0.3, \dots, 0.9, 1.0$. γ increases in the direction of the arrow.

To investigate firing rates in the fractional cable models we consider solutions to Eqs. (14) and (15) with $\frac{\partial^2 V}{\partial X^2} = 0$ for a homogeneous membrane patch, and with a constant externally applied current density i_e . The solutions are

$$V_I(T) = i_e r_m + (V_o - i_e r_m) \exp(-\mu^2 T^\kappa), \quad (18)$$

$$V_{II}(T) = i_e r_m + (V_o - i_e r_m) E_\kappa(-\mu^2 T^\kappa), \quad (19)$$

where V_o is the initial potential. The solutions are similar at short times where the Mittag-Leffler function $E_\kappa(z)$ behaves like a stretched exponential [13], and at long times both solutions decay to the steady state $V = i_e r_m$. In both models, the firing rate obtained by incorporating the solutions in a simple passive integrate and fire model is well approximated by [23]

$$\frac{1}{T_{\text{fire}}} \sim \left[\frac{1}{\mu^2} \ln \left(\frac{i_e r_m - V_r}{i_e r_m - V_t} \right) \right]^{-1/\kappa}, \quad (20)$$

where V_t is the threshold potential for the cell to fire and V_r is the reset potential after firing. The anomalous diffusion does not affect the threshold current for nerve cell firing, $i_e > V_t/r_m$, but it does impact on firing rates.

The fractional electrodiffusion models considered in this Letter offer new cable equations for spiny neurons where the spines trap and release diffusing molecules resulting in anomalously slow diffusion. The additional scaling exponent parameters appearing in temporal operators in these equations enable predictions that cannot be obtained from the standard cable equation with existing parameters adjusted to accommodate spines. The linear fractional cable models, which both predict similar qualitative behaviors, could be calibrated and validated through electrophysiological experiments. From Eq. (18), or Eq. (19), with $V_o = 0$, the parameters r_m, μ, κ could be fit to the time course of the membrane potential from a patch recording in response to a hyperpolarizing current $i_e < 0$. Assuming standard values for c_m , and $\kappa = \gamma$ in steady state, $r_L(\gamma)$ could be obtained from steady state voltage attenuation measurements using simultaneous patch-pipette recordings [28] from the soma and the apical dendrite of a pyramidal neuron. The model prediction for the different arrival times at the soma of dendritic postsynaptic potentials as a func-

tion of spine density could be investigated qualitatively through measurements of the time course of potentials at the soma in response to currents applied in apical and basal trees, where spine densities are different.

This research was supported by the Australian Commonwealth Government ARC Discovery Grants Scheme and NIH grants from NIMH and NIDCD, U.S.A.

*B.Henry@unsw.edu.au

†t.langlands@unsw.edu.au

*susan.wearne@mssm.edu

- [1] I. Segev and M. London, *Science* **290**, 744 (2000).
- [2] W. Rall, *Exp. Neurol.* **1**, 491 (1959).
- [3] W. Rall, in *Handbook of Physiology: The Nervous System*, edited by R. Poeter (American Physiological Society, Bethesda, MD, 1977), Vol. 1, Chap. 3, pp. 39–97.
- [4] N. Qian and T.J. Sejnowski, *Biol. Cybern.* **62**, 1 (1989).
- [5] A. Matus and G.M. Shepherd, *Neuron* **27**, 431 (2000).
- [6] E.A. Nimchinsky, B.L. Sabatini, and K. Svoboda, *Annu. Rev. Physiol.* **64**, 313 (2002).
- [7] J. Bourne and K.M. Harris, *Curr. Opin. Neurobiol.* **17**, 381 (2007).
- [8] G.J. Stuart and B. Sakmann, *Nature (London)* **367**, 69 (1994).
- [9] C. Koch, *Biophysics of Computation, Information Processing in Single Neurons, Computational Neuroscience* (Oxford University, New York, 1999).
- [10] S.M. Baer and J. Rinzel, *J. Neurophysiol.* **65**, 874 (1991).
- [11] F. Santamaria, S. Wils, E. De Schutter, and G.J. Augustine, *Neuron* **52**, 635 (2006).
- [12] K.G. Wang, *Phys. Rev. A* **45**, 833 (1992).
- [13] R. Metzler and J. Klafter, *Phys. Rep.* **339**, 1 (2000).
- [14] H. Scher and E. Montroll, *Phys. Rev. B* **12**, 2455 (1975).
- [15] M.J. Saxton, *Biophys. J.* **81**, 2226 (2001).
- [16] E. Lutz, *Phys. Rev. E* **64**, 051106 (2001).
- [17] R. Metzler, J. Klafter, and I.M. Sokolov, *Phys. Rev. E* **58**, 1621 (1998).
- [18] E. Barkai, R. Metzler, and J. Klafter, *Phys. Rev. E* **61**, 132 (2000).
- [19] E. Heinsalu, M. Patriarca, I. Goychuk, and P. Hänggi, *Phys. Rev. Lett.* **99**, 120602 (2007).
- [20] H.C. Tuckwell, *Introduction to Theoretical Neurobiology* (Cambridge University Press, Cambridge, England, 1988), Vol. 1.
- [21] I.M. Sokolov, A. Blumen, and J. Klafter, *Physica (Amsterdam)* **302A**, 268 (2001).
- [22] I.M. Sokolov, *Phys. Rev. E* **63**, 056111 (2001).
- [23] T.A.M. Langlands, B.I. Henry, and S.L. Wearne (to be published).
- [24] B.I. Henry, T.A.M. Langlands, and S.L. Wearne, *Phys. Rev. E* **74**, 031116 (2006).
- [25] B. Jacobs, L. Driscoll, and M. Schall, *J. Comp. Neurol.* **386**, 661 (1997).
- [26] H. Duan, S.L. Wearne, A.B. Rocher, A. Macedo, J. Morrison, and P.R. Hof, *Cereb. Cortex* **13**, 950 (2003).
- [27] M. Suetsugu and P. Mehraein, *Acta Neuropathol.* **50**, 207 (1980).
- [28] G. Stuart and N. Spruston, *J. Neurosci.* **18**, 3501 (1998).